

## THRESHOLD DRIFTS OF STRUCTURAL PERFORMANCE LEVELS IN DUCTILITY-LIMITED WALLS WITH DUCTILE MESH


### PRAGOVI POMERANJA NIVOVA KONSTRUKCIONOG IZVOĐENJA ZIDOVA OGRANIČENE DUKTILNOSTI SA DUKTILNOM MREŽOM

Originalni naučni rad / Original scientific paper


Rad primljen / Paper received: 11.11.2022

<https://doi.org/10.69644/ivk-2024-03-0360>

Adresa autora / Author's address:

<sup>1)</sup> Universidad Católica Santo Toribio de Mogrovejo, Chiclayo, Peru  
J.A.A. Martínez  0000-0003-4154-9510;

\*email: [rcaleroarboza@gmail.com](mailto:rcaleroarboza@gmail.com)

<sup>2)</sup> Universidad Nacional Toribio Rodríguez de Mendoza de Amazonas, Peru  
Á.A.Riuz-Pico  0000-0003-2638-0593

#### Keywords

- drifts
- trilinear curve
- post-elastic
- post-cracking
- post-creep

#### Abstract

*This paper presents the experimental results performed by SENCICO, based on cyclic loads that were applied to 03 walls of limited ductility brought to failure in laboratory tests. These results were evaluated and processed in order to analyse their performance under controlled lateral loading conditions, to obtain their hysteretic loops representing their stiffness degradation in 13 proposed phases. In turn, the enveloping capacity curves were determined for each specimen in order to obtain a representative curve for the samples. Subsequently, the representative curve is validated through a theoretical calibration with the help of the ETABS<sup>®</sup> software, adding the nonlinearity to the materials and the mathematical model, obtaining an analytical capacity curve very similar to the experimental one. In addition, a trilinear curve is proposed that fits accurately and represents very well the performance of walls with limited ductility in their elastic, post-cracking and post-creep performance conditions. Finally, the trilinear capacity curve is sectorized in its structural performance levels with their respective threshold drifts, guided by the guidelines proposed by SEAOC VISION 2000.*

#### INTRODUCTION

In the last decade, the trend towards national population growth and development in the world has been remarkable. As a consequence of this growth, the need for housing in the country has increased. For this reason, reinforced concrete buildings of low and medium height (5-7 stories), mainly made up of walls and slabs, are a technical-efficient option in terms of low economic cost. Limited ductility walls are used in these constructions with usual thicknesses of 8 and 10 cm with a reinforcing steel mesh /1/.

The limited ductility wall system is a construction technology that has rapidly obtained wide acceptance in comparison to the most commonly used traditional systems due to its economic advantage and high speed of construction. However, low ductility, scarce experimental information, lack of background information on structural performance under large magnitude earthquakes, and the lack of quality

#### Ključne reči

- pomeranja
- trilinearna kriva
- post-elastično
- post-prslina
- post-puzanje

#### Izvod

*U radu su prikazani eksperimentalni rezultati koje je sproveo SENCICO na osnovu cikličkih opterećenja primenjenih na 03 zidove ograničene duktilnosti, koji su dovedeni do loma u laboratorijskim ispitivanjima. Ovi rezultati su dobijeni procenom i obrađeni su za analizu ponašanja zidova u uslovima kontrolisanog bočnog opterećenja, za dobijanje njihove histerezisne petlje, koje predstavljaju degradaciju njihove krutosti u 13 predloženih faza. Zauzvrat, obuhvatne krive kapaciteta su određene za svaki uzorak da bi se dobila reprezentativna kriva uzoraka. Nakon toga, reprezentativna kriva se proverava teorijskom kalibracijom pomoću softvera ETABS<sup>®</sup>, dodavanjem nelinearnosti materijalima i matematičkom modelu, čime se dobija analitička kriva kapaciteta vrlo slična eksperimentalnoj. Predlaže se trilinearna kriva koja se precizno prilagođava koja veoma dobro predstavlja ponašanje zidova ograničene duktilnosti u uslovima elastičnog ponašanja post-prslina i post-puzanja. Konačno, trilinearna kriva kapaciteta je podeljena na nivoe strukturalnih performansi sa odgovarajućim pragom pomeranja, shodno smernicama koje predlaže SEAOC VISION 2000.*

control in the construction process have led to the fact that these buildings are susceptible to medium and high intensity earthquakes. For this reason, this paper studies the structural performance in the plane of limited ductility walls, /2/.

The study is carried out by means of the construction of three full-scale walls with the same dimensions and characteristics, subjected to cyclic lateral loads until failure. The test is constituted by applying controlled displacements at the top of each specimen following the guidelines regulated by The Structural Laboratory Facilities of Pontificia Universidad Católica del Perú are used for the construction and data collection, /4/.

The result found from the cyclic tests are the hysteresis loops whose graphs will help to generate maximum force vs. displacement envelopes which are the capacity curves in their positive and negative range; from which the representative capacity curve is statistically determined, whose performance is validated by means of a calibration in a

mathematical model generated in ETABS v.20 with the assignment of the nonlinearity of the materials as well as their physical and mechanical characteristics, these results will be used to determine the control points that form a trilinear capacity curve constituted by three slopes that represent the elastic stiffness, post-cracking stiffness, and post-creep stiffness, up to the maximum resistance as shown in (Fig. 1), /4/.

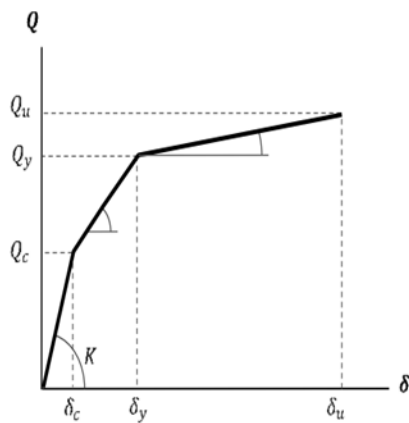


Figure 1. Trilinear curve, /4/.

Likewise, the mechanical characteristics of the specimens such as ductility, strength and stiffness are obtained from this graph in order to determine the levels of structural performance or damage as a function of the limit drifts.

PHYSICAL AND MECHANICAL CHARACTERISTICS OF THE SPECIMENS

Material characteristics

- Reinforcing steel

For specimens, grade 60 steel established under the guidelines of ASTM A 615 is used.

Table 1. Characteristics of A615 Steel.

Characteristics	Value		ASTM A615
Minimum yield strength (fy)	4200 kg/cm <sup>2</sup>		comply
Minimum tensile strength (fu)	6300 kg/cm <sup>2</sup>		comply
Modulus of elasticity E	2000000 kg/cm <sup>2</sup>		not specified
Deformation at onset of creep (ey)	0.0021		comply
Minimum lengthening at break	Diameter	Minimum elongation at break	comply
	3/8", 1/2", 5/8", 3/4"	9 %	
	1"	8 %	
	1 3/8"	7 %	

Source: Experimental tests of limited ductility walls

- Concrete

The concrete used in the construction of the walls varied according to the functionality of the structural element. The concrete for the foundation beams was designed with a characteristic strength of 210 kg/cm<sup>2</sup> by Fuller's method, taking into account the properties of the aggregates in the laboratory. Ready-mix concrete was used for the walls and floor beams. The order indicated that the concrete was for walls

of limited ductility, so ASTM C-33 spindle 67 for the coarse aggregate, concrete compressive strength 175 kg/cm<sup>2</sup>, 6" slump and additionally polypropylene fibres were used. Table 2 below shows the technical specifications considered for the concrete.

Table 2. Concrete technical specifications.

TECHNICAL SPECIFICATIONS	
Compressive strength Fc at 28 days old	175 a 210 kg/cm <sup>2</sup> , as established by the project designer.
Coarse aggregate	Maximum Nominal Size 1", to comply with HUSO 57 AST C-33 (Smaller T.M. may be used at builder's criterion, but not bigger than specified).
Fine aggregate	Granulometry according to ASTM C-33
Type of cement	It can be Standard according to ASTM C-150 (Type I, II, V) or Additivated according to ASTM C-595, being able to be used mineral additions, as established by the project designer for durability criteria.
Prolipropyrene fibers	400 gr to 900 gr, as established by the project designer.
Slump (in.)	3 to 4 inches minimum
Incorporated air in %	3% to 4%

Materials testing

- Reinforced steel

Samples of the steel used in the construction of the walls were taken for tensile testing of the steel. Tensile testing of steel bars was performed in accordance with ASTM A370. 6 specimens were tested for each rebar diameter (1/2" and 3/8"). The tensile test was performed in the MTS Universal Testing Machine, which applies an axial load to the specimen and allows measuring the applied load and deformation generated in the specimen (Fig. 2).



Figure 2. Placement of specimen in the jaws of universal machine. Tested specimens of 3/8" samples.

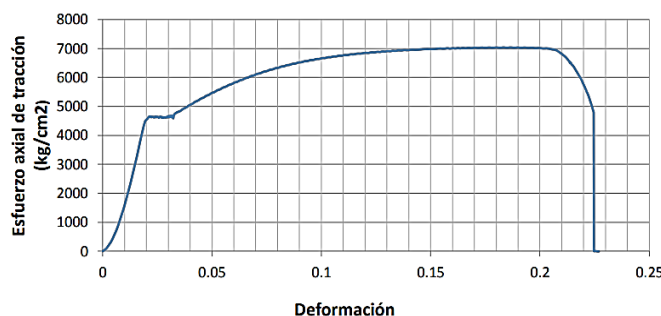


Figure 3. Global stress-strain diagram for 3/8" sample, specimen 1.

The specimens were placed one by one in the Universal Machine cell. The steel bars upon reaching breakage released energy in the form of heat. In the overall stress-strain graphs for the 3/8" (Fig. 3) and 1/2" (Fig. 4) specimen, the small creep platform and the hardening process of the steel are observed.

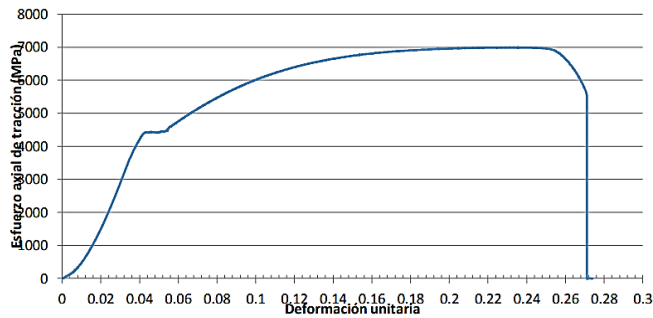


Figure 4. Global stress-strain diagram of 1/2" sample, specimen 6.

Tables 3 and 4 are presented below with the summary of yield stresses (fy) and ultimate stresses (fu) of the six steel specimens tested.

Table 3. 3/8" reinforcing steel specimens.

Sample	fy	fu	fu/fy
Specimen 1	4635	7035	1.52
Specimen 2	4460	7063	1.58
Specimen 3	4520	7062	1.56
Specimen 4	4590	7040	1.53
Specimen 5	4490	7060	1.57
Specimen 6	4600	7097	1.54

Source: Limited ductility walls experimental tests.

Table 4. 1/2" reinforcing steel samples.

Sample	fy	fu	fu/fy
Specimen 1	4415	7001	1.59
Specimen 2	4535	7258	1.60
Specimen 3	4440	7006	1.58
Specimen 4	4425	6997	1.58
Specimen 5	4530	7280	1.61
Specimen 6	4420	6992	1.58

Source: Limited ductility walls experimental testing

- Concrete



Figure 5. Production of concrete specimens.



Figure 6. Specimen tested in axial compression.

A total of 22 concrete specimens are produced (Fig. 5). The prepared specimens were demolded the day after casting and placed in the curing pond. Two specimens were tested seven days after casting, two specimens were tested at twenty-eight days and the remaining two were tested on the same day as the wall test (Fig. 6).

Table 5 below shows the specimens tested and their compressive strength.

Table 5. Compressive strength of concrete specimens in walls and floor beams.

Specimen	Design strength	Age (days)	Diameter		Maximum Load (KN)	Type of failure	Stress (kg/cm2)	% of resistance	Average stress (kg/cm2)	% of average resistance
			D1	D2						
M-MDL+N°01	175	7	152.9	154	311.8	2	172.31	98.46	170	97.14
M-MDL+N°02			154.5	154	308	2	167.69	95.82		
M-MDL+N°03	175	21	153.6	154	380.8	3	209.62	119.78	211.05	120.6
M-MDL+N°04			151.6	152	376	2	212.48	121.42		
M-MDL+N°05	175	28	152.6	152	374.7	5	209.25	119.78	202.17	115.53
M-MDL+N°06			152.5	153	351.4	2	195.09	111.48		
M-MDL+N°07	175	31	154	154	380.8	2	209.08	119.57	215.06	122.89
M-MDL+N°08			153	151	394	4	221.04	111.48		
M-MDL+N°09	175	33	154	152	382	2	212.08	119.47	196.57	112.89
M-MDL+N°10			157.7	158	346.5	2	181.06	126.31		
M-MDL+N°11	175	35	153.9	154	311.8	2	213.09	121.19	215.71	123.26
M-MDL+N°12			154.5	154	308	2	218.32	103.47		
M-MDL+N°13	175	39	155.4	155	415.3	2	223.78	121.77	222.08	126.9
M-MDL+N°14			153.8	153	400.6	2	220.38	125.93		
M-MDL+N°15	175	40	153	152	404.6	2	225.21	128.69	217.58	124.33
M-MDL+N°16			152.3	153	376.7	2	209.96	119.97		
M-MDL+N°17	175	76	152.5	153	430	2	239.04	136.59	241.11	137.78
M-MDL+N°18			153.6	153	441.2	3	243.19	138.96		
M-MDL+N°19	175	77	149.3	149	445.3	2	259.46	148.26	257.59	147.19
M-MDL+N°20			147.5	146	424.3	4	255.72	146.12		
M-MDL+N°21	175	81	146.9	147	408.5	5	245.19	140.11	231.85	132.48
M-MDL+N°22			147	147	363.3	2	218.51	124.86		

Source: Experimental tests on walls of limited ductility.

Description of the specimens

The three (03) specimens were tested without vertical load and with lateral load until failure, the walls were anchored to foundation beams of 0.44 m high x 0.25 m wide, in each wall a 0.25 m wide and 0.20 m high beam was placed, the steel distribution in the web was every 25 cm a 3/8" steel and in the edges 3 1/2" steels, Fig. 7.

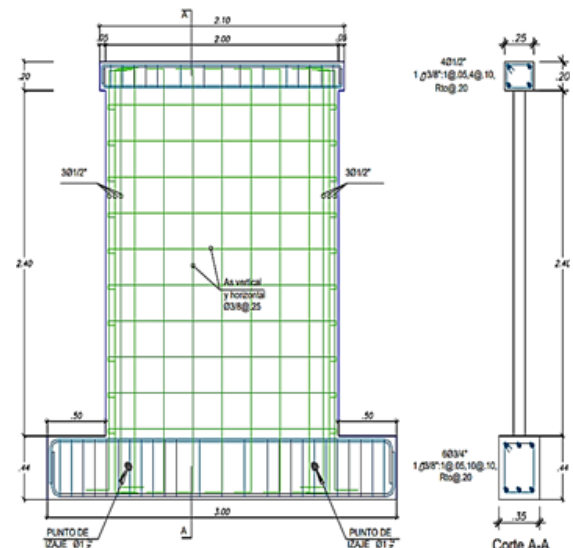


Figure 7. Structural detail of specimens.

Testing technique

The cyclic lateral load test followed the guidelines of FEMA 461 and was developed in the structures laboratory of Pontificia Universidad Católica del Perú. FEMA 461 presents recommendations for the test procedure, load history



and guidelines for estimating the performance of structural elements of a building using quasi-static cyclic tests.

Figure 8 presents a conceptual diagram of the recommended load history. The load history consists of repeated cycles with stepwise increasing strain amplitudes. Two cycles will be completed per phase.

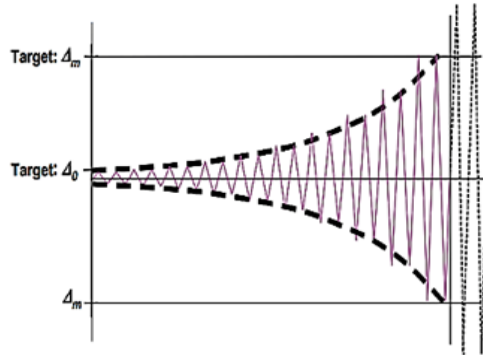


Figure 8. Load history diagram with controlled deformation (FEMA-461, 2007).

- $\Delta_0$  = Minimum amplitude. It should be sufficiently less than the amplitude at which the first damage state is expected to initiate. When the first damage state occurs, at least six loading cycles must have been performed.
- $\Delta_m$  = Maximum amplitude. This should be an estimated value at which the most severe damage state is expected to initiate. This value should be estimated prior to testing. If during the test, the most severe damage state has not occurred at the expected amplitude, incremental amplitudes of  $0.3 \Delta_m$  should still be applied. □
- $n$  = Number of phases (or increments) of the test, will generally be 10 or more.
- $a_i$  = Amplitude of phase  $i$ . The first amplitude at 1 will be  $\Delta_0$  and the last amplitude will be  $\Delta_m$ . The test should continue above the maximum value  $\Delta_m$  until the maximum capacity of the

The amplitude  $a_{i+1}$  of phase  $i+1$  (not of each cycle, since each phase has two cycles) is given by the following equation:  $a_{i+1} = 1.4a_i$ .

Thirteen lateral load phases are proposed for each specimen test. Each phase for each wall corresponds to the same displacement in order to be able to compare the performance of the 3 walls. The increment per phase is performed following the recommendations of FEMA 461. Table 6 shows

Phase	MDL-01	MDL-02	MDL-03
1	Disp 0.50 mm Late 5.49 Tonf <i>Observation:</i> The specimen did not show cracks and had an elastic performance.	Disp 0.50 mm Late 4.80 Tonf <i>Observation:</i> The specimen did not show cracks and had an elastic performance.	Displa.50 mm Latera.2 Tonf <i>Observation:</i> The specimen did not show cracks and had an elastic performance.
11	Disp 16.50 mm Late 25.35 Tonf <i>Observation:</i> Existing cracks were lengthened and others only increased in thickness to 0.80 mm. others only increased in thickness up to 0.80 mm. At the base, slippage of the wall with respect to the foundation beam was observed."	Disp 16.50 mm Late 22.90 Tonf <i>Observation:</i> Existing cracks were lengthened and others only increased in thickness to 0.80 mm. others only increased in thickness up to 0.80 mm. At the base, slippage of the wall with respect to the foundation beam was observed."	Displa.50 mm Latera.62 Tonf <i>Observation:</i> Existing cracks were lengthened and other cracks only increased in thickness up to 0.50 mm. Diagonal tensile cracks with a thickness of less than 0.50 mm appeared.
12	Disp 23.50 mm Late 26.44 Tonf <i>Observation:</i> Existing cracks lengthened and others only increased in thickness; at the lower ends, the thickness of existing cracks increased by up to 2 mm.	Disp 23.50 mm Late 24.27 Tonf <i>Observation:</i> Diagonal tensile cracks with a maximum thickness of 0.40 mm appeared. Existing cracks were lengthened and other cracks only increased in thickness; at the lower ends, the thickness of existing cracks increased to more than 1 mm. Crushing of the heels was observed.	Displa.50 mm Latera.76 Tonf <i>Observation:</i> Existing cracks were lengthened and others only increased in thickness; at the lower ends, the thickness of existing cracks increased to a maximum value of 1.5 mm; crushing of the heels was observed.
13	Disp 30.50 mm Late 26.35 Tonf <i>Observation:</i> Crushing was observed at the interior ends of the wall.	Disp 30.5 mm Late 24.79 Tonf <i>Observation:</i> Severe crushing of the heels and buckling of the vertical steel at the lower left end of the wall was observed.	Displa.50mm Latera.16 Tonf <i>Observation:</i> Severe crushing of the left heel was observed.

the phases used for the CDMs.

Likewise, Fig. 9 shows the lateral displacement history imposed on the CDM walls.

Table 6. Cyclic test phases.

PHASE	1	2	3	4	5	6	7	8	9	10	11	12	13
Drift (%)	0.20	0.35	0.42	0.63	0.83	1.25	1.88	2.50	3.54	5.00	6.88	9.80	12.71
Displacement (mm)	0.50	0.80	1.00	1.50	2.00	3.00	4.50	6.00	8.50	12.00	16.50	23.50	30.50

Source: Experimental tests of limited ductility walls, SENCICO.

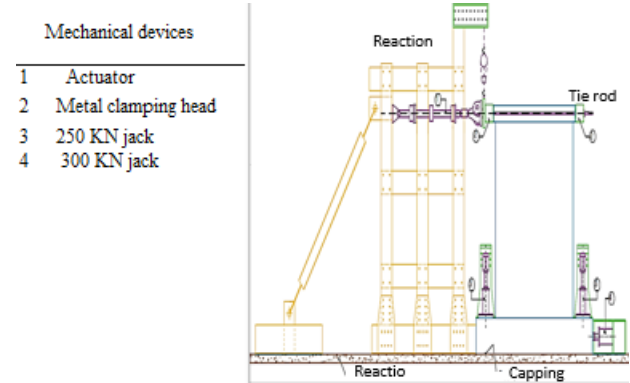


Figure 9. Complete system for the application of cyclic lateral load.

### QUALITATIVE PERFORMANCE OF LIMITED DUCTILITY WALLS

The specimens had an elastic performance in the first phase of the test, in the following phases they presented flexural failures with cracks that varied from 0.05-0.15 mm, in addition, in the last and penultimate phase there was failure due to sliding and crushing of the wall heels and buckling of the vertical steel, respectively. Table 7 describes the qualitative performance of specimens in each representative phase of the test.

Table 7. Qualitative description of structural performance of specimens.

Likewise, a post-test inspection was carried out, evidencing the buckling of vertical reinforcing steels.

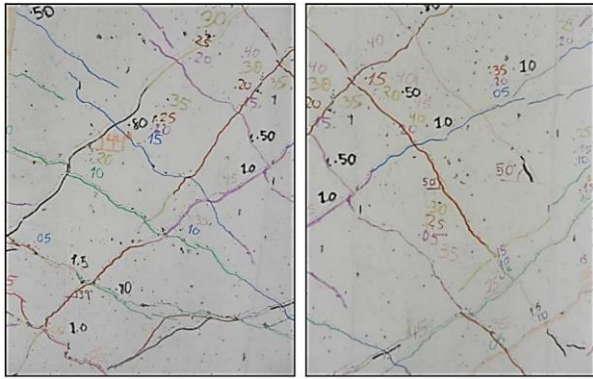


Figure 10. Diagonal failures by bending.



Figure 11. Buckling in reinforcing steel.

HYSTERESIS LOOPS AND SHEAR FORCE ENVELOPE

Figure 12 shows graphs corresponding to hysteresis loops for three samples. It can be seen that hysteresis loops reflect the stiffness degradation on the negative side of each hysteresis cycle due to the tensile stresses caused by lateral loading and unloading in the specimen.

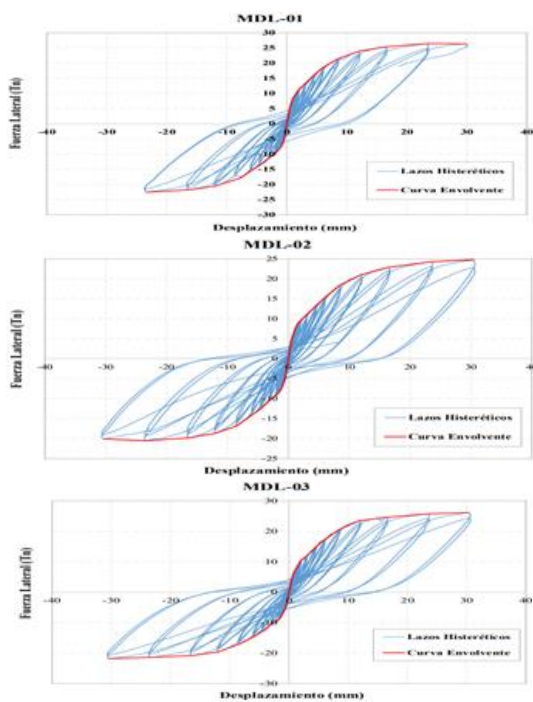


Figure 12. Hysteresis loops.

ENVELOPING CAPACITY CURVES AND REPRESENTATIVE CURVE OF THE THREE SPECIMENS

The envelopes of positive and negative capacity curves generated by wall, i.e., CDM 01, 02, and 03, were made taking into account the maximum force and displacement per cycle, and the average curve is calculated for each specimen, as shown in Fig. 13.

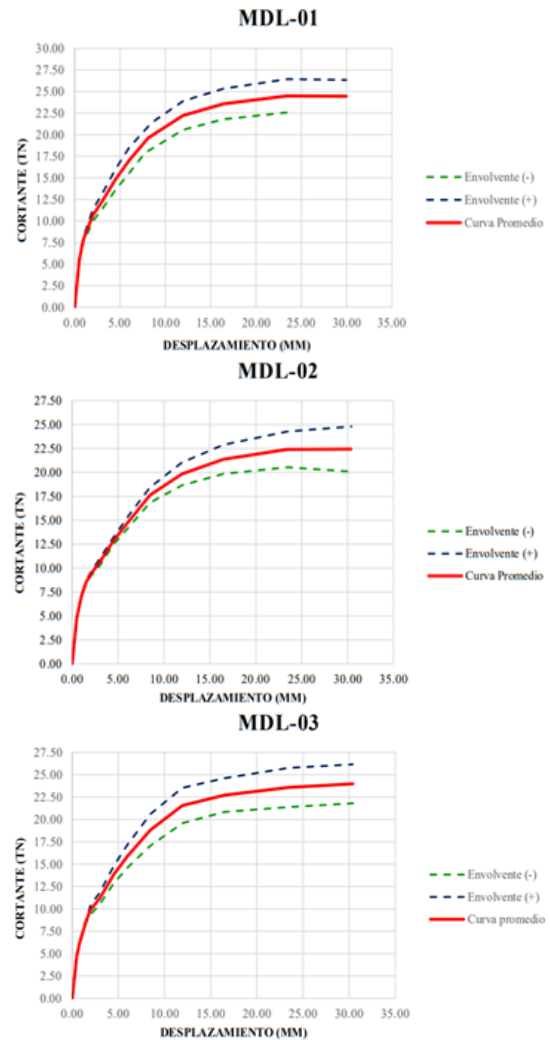


Figure 13. Average capacity curves.

Curva de capacidad Representativa MDL 01,02 y 03

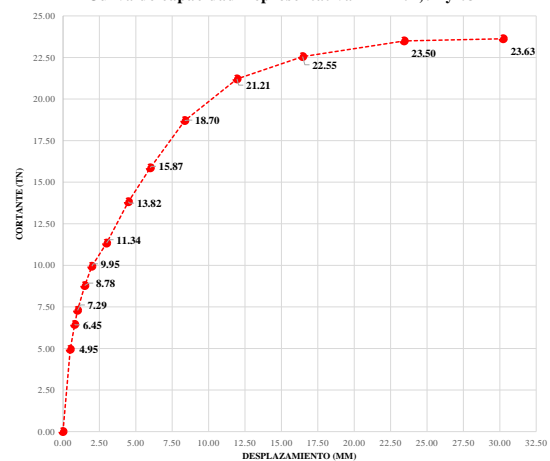


Figure 14. Representative curve.

In the same way, the average curves of the three ductility limited walls are statistically processed and 50 % structural reliability is considered to determine the force vs. displacement representative of the three samples. Figure 14 shows the average shears for the average displacements in (mm) of 0.5; 0.80; 1; 1.49; 1.98; 3; 4.50; 5.99; 8.36; 11.95; 16.46; 23.43, and 30.24, respectively.

**VALIDATION OF THE REPRESENTATIVE CURVE BY MEANS OF A MATHEMATICAL MODEL**

Validation of the representative capacity curve is performed by means of an analytical mathematical model in ETABS® software considering its structural configuration, geometry, constituent materials, and the average control displacements obtained in the representative capacity curve.

*Geometric representation of the mathematical model.*

As specified in the description of the specimen, a wall height of 2.40 m by width of 2 m is considered, discretizing vertically for the correct allocation of steel reinforcement at the edges and in the core.

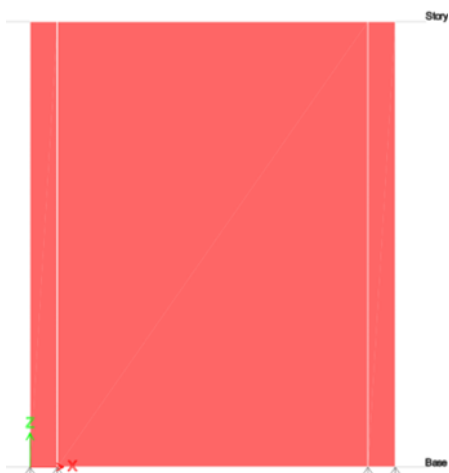


Figure 15. Discretized mathematical model.

*Assignment of Nonlinearity to Materials*

**- Steel reinforcement**

Steel constitutive diagrams are considered as indicated in experimental data from materials testing of the reinforced steel, which consists of assigning the stress-strain characteristics obtained in the tests to the 3/8" and 1/2" reinforcing steel as shown in Fig. 16.

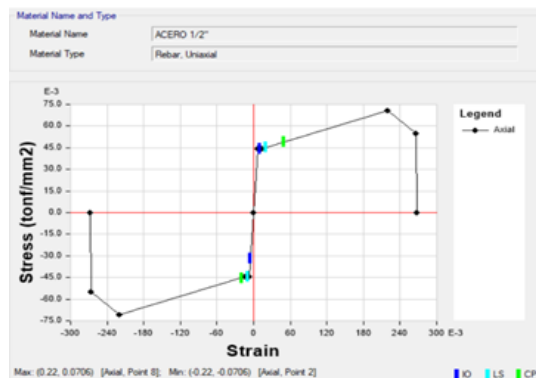
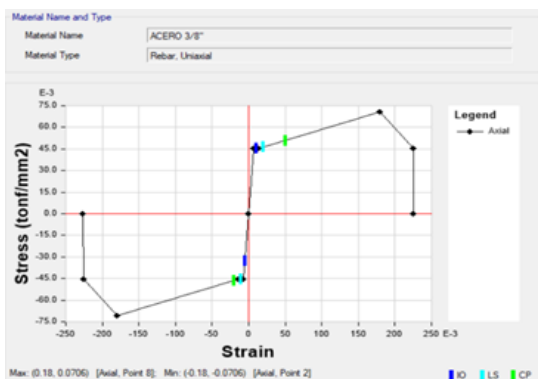


Figure 16. Constitutive models, 3/8" and 1/2" steel.

**- Concrete**

In the constitutive diagram of concrete, the model proposed by Hognestad is used, which recommends an initial unit deformation of 0.002 and a final unit deformation of 0.0038 for conventional concrete, at the same time it considers that compressive stress of concrete can be reduced by up to 85 %, for the present article these proposed parameters are used in order to better resemble the theoretical capacity curve to the experimental one, as shown in Fig. 17, the Hognestad's model inserted into the constitutive model of concrete in the ETABS software.

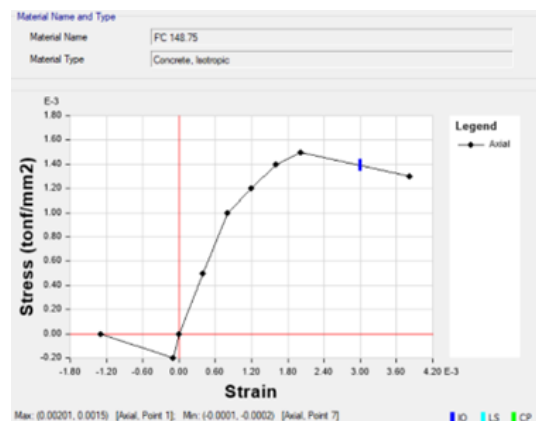


Figure 17. Concrete constitutive model.

*Assignment of the amount and fibre-type plasticity*

Structural configuration of the representative specimen considers the distribution of reinforcing steel, the amounts at the edge and in the core of 3/8" and 1/2", respectively, and the wall hinge is assigned in its fibre type condition for the correct nonlinear reading of the model. Then, the nonlinear monotonic load condition is applied with an average displacement control of 29.9 mm (Fig. 18).

*Model discretization: stiffness degradation*

Within the analytical calibration parameters, the stiffness degradation of the mathematical model is considered by means of horizontal and vertical discretization applying the finite element criterion to properly resemble the experimental curve to the analytical curve, Fig. 19.

*Experimental vs. analytical calibrated capacity curve*

Once the correct discretization of the mathematical model is completed, a Pier label is assigned to the section for the

correct reading of shear force at the base, then the software is run, and the capacity curve is evaluated with the actual assigned displacement control of 29.9 mm. Figure 20 shows the analytical vs. experimental capacity curve whose performance slopes in its elastic and inelastic state are very well matched.



Figure 18. Fiber-type quantum and plasticity.

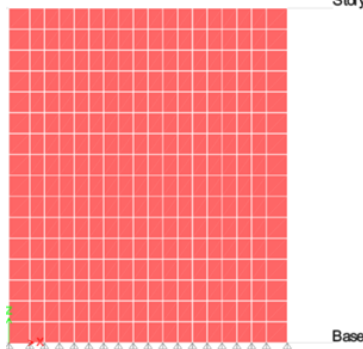


Figure 19. Horizontal and vertical discretization.

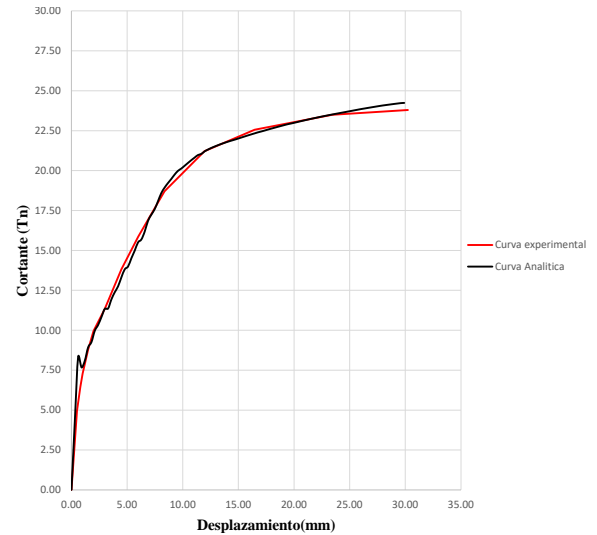


Figure 20. Analytical vs. experimental curve.

- Elastic performance (elastic stiffness): it is characterised by presenting flexural cracks located in the heel zone of the wall that establishes initiation of cracking. It is estimated that maximal thickness of cracks is 0.05 mm, /3/.
- Post-cracking stiffness: after the first cracking appears, diagonal shear cracks with maximum thickness of 2 mm appear. At the same time, there is a considerable degradation of stiffness. In addition, crushing of the concrete in the heel area begins, /3/.
- Post-creep stiffness: in this state of damage, the ultimate strength of the walls is reached. The thickness of diagonal cracks increases up to 3 mm, the crushing of concrete is aggravated, there is shear displacement at the base of the wall and buckling of steel bars in the heel zone is observed, compromising the stability of the wall, /3/.

Such considerations are represented at three points on the capacity curve. These are average values of shear and displacements in phase 6 (Table 7), phase 11 (Table 8), and phase 13 (Table 9), respectively. The trilinear capacity curve is then sampled in Fig. 21.

TRILINEAR CAPACITY CURVE

The capacity curve of a ductility-limited wall can be symbolized by a trilinear capacity curve. The trilinear curve is expressed by three different slopes, which represent elastic stiffness, post-cracking stiffness, and post-creep stiffness, until reaching the maximum resistance /4/, in this way a description of remarkable points and the damage of ductility-limited walls at each point could be made.

For the representation of the trilinear capacity curve, the following considerations are used.

Table 7. Elastic stiffness.

Cortante y desplazamiento				FASE 6			
Muros	Comportamiento elastico (rigidez elastica)						
	Envolvente (-)		Envolvente (+)		Promedio		
	V(Tnf)	D(mm)	V(Tnf)	D(mm)	V(Tnf)	D(mm)	
MDL-01	11.32	2.99	13.09	3.00	11.34	3.00	
MDL-02	10.23	2.99	10.98	3.00			
MDL-03	10.54	2.99	11.86	3.00			

Table 8. Post cracking stiffness.

Cortante y desplazamiento				FASE 11			
Muros	Rigidez post agrietamiento						
	Envolvente (-)		Envolvente (+)		Promedio		
	V(Tnf)	D(mm)	V(Tnf)	D(mm)	V(Tnf)	D(mm)	
MDL-01	21.79	16.41	25.35	16.44	22.55	16.46	
MDL-02	19.84	16.45	22.90	16.50			
MDL-03	20.83	16.47	24.62	16.48			

Table 9. Post creep stiffness.

Cortante y desplazamiento				FASE 13			
Muros	Rigidez post fluencia						
	Envolvente (-)		Envolvente (+)		Promedio		
	V(Tnf)	D(mm)	V(Tnf)	D(mm)	V(Tnf)	D(mm)	
MDL-01	22.57	0.00	26.35	29.94	23.63	30.30	
MDL-02	20.09	30.33	24.79	30.40			
MDL-03	21.81	30.43	26.16	30.39			



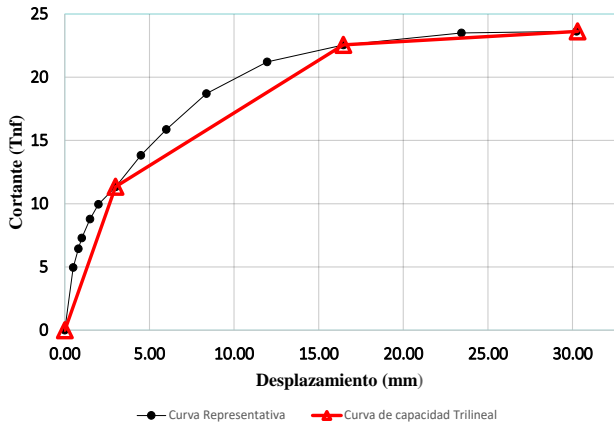


Figure 21. Trilinear plot of the capacity curve.

The three points representing the trilinear graph are defined as creep, post-cracking, and post-creep.

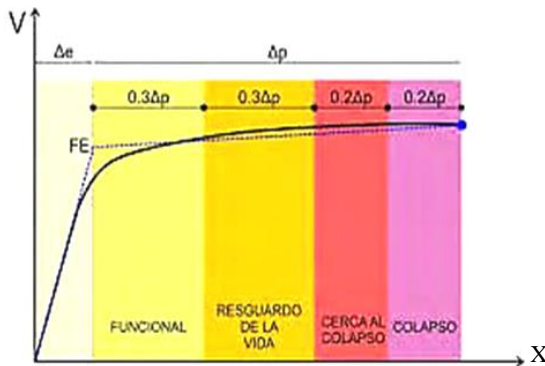


Figure 22. Sectorization according to SEAOC VISION 2000.

To describe and represent the structural performance produced in the limited ductility walls, limit drifts are determined for 5 levels of damage, whose damage levels are calculated according to guidelines recommended by SEAOC VISION 2000, which indicates that from the plastic or inelastic displacement ( $\Delta p$ ) should be divided into 30 %  $\Delta p$  for functional limit and life safety, and 20 %  $\Delta p$  for near collapse and collapse.

These areas are divided according to performance level limits of a wall structure with limited ductility (Fig. 23).

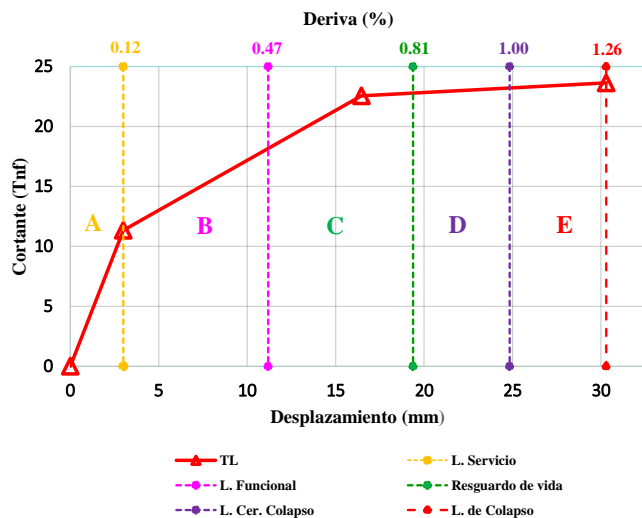


Figure 23. Threshold drifts of performance levels.

CONCLUSIONS

Elastic performance is identified in the first 6 phases of the test with a representative shear of 11.4 Tonf for an average displacement of 3 mm.

A shear of 22.55 and 23.63 Tonf is found for displacements 16.46 and 30.30 mm, representing a performance of post-cracking stiffness and post-creep stiffness, respectively.

The sectorization is determined according to the failure modes that represent the types of behaviour for the structural performance limits as detailed below:

- Zone A: the wall has an elastic performance. The loading and unloading of the force applied to the specimen is maintained on the straight line described in this zone. The damages produced to the wall are mostly flexural tensile cracks, as well as the beginning of the appearance of horizontal cracks in the part of the heels.
- Zone B: the post-cracking stage begins, in which the stiffness value is not the same as the initial one. The damage in this stage is the formation of pure tensile cracks in the wall with an average thickness of 0.15 mm.
- Zone C: it is still maintained in the post-cracking stage. Damages produced in this stage are increase in the thickness of diagonal pure tensile cracks which are between 0.5-0.80 mm.
- Zone D: in this zone the post-cracking stage ends and starts when there is a significant change in the slope following the capacity curve. The post-creep stage begins. Damage in this zone is characterised by diagonal shear cracks with an average thickness of 2 mm, in addition to the beginning of the crushing of the concrete at the heels of the wall.
- Zone E: the wall develops a final resistance. It is observed that the wall is close to collapse, and there is evidence of buckling of longitudinal reinforcing steels, failure due to sliding of the wall and total detachment of concrete at the wall heels, compromising the overall stability of the wall.

Threshold drift levels are obtained for different types of performance levels A, B, C, D, and E, drifts of 0.12 %; 0.47 %; 0.81 %; 1 %, and 1.26 %, respectively.

REFERENCES

1. López, G., Verduga, J., *Seismic risk assessment of limited ductility structures in the parish of Alóag, province of Pichincha*, Central University of Ecuador, 2019. (in Spanish)
2. Vélez, J., Blandón, C.A., Bonett, R., et al., *Cyclic quasi-static testing of thin reinforced concrete walls in Colombian buildings*, Colombian Earthquake Engineering Research Center - CEER. (in Spanish)
3. Acero, J., *Structural testing services to determine the seismic behavior of limited ductility walls*, Pontificia Universidad Católica del Perú, Lima, Perú, 2016. (in Spanish)
4. Quezada, S., *Most common failures in structural systems of limited ductility in houses of up to two floors in high seismic zones*, University of Machala, Machala, 2019. (in Spanish)
5. Díaz, M., *Review of design criteria for buildings with limited ductility walls, established in Peruvian structural standards and proposal for updating*, Perú, 2021. (in Spanish)

© 2024 The Author. Structural Integrity and Life, Published by DIVK (The Society for Structural Integrity and Life 'Prof. Dr Stojan Sedmak') (<http://divk.inovacionicentar.rs/ivk/home.html>). This is an open access article distributed under the terms and conditions of the Creative Commons Attribution-NonCommercial-NoDerivatives 4.0 International License